Jo et al. Ecological Processes (2026) 15:11
https://doi.org/10.1186/s13717-026-00670-z

Ecological Processes

RESEARCH Open Access

Disentangling variation patterns and partitioning strategies of net primary productivity: insights from cool-temperate forests in South Korea

Min Seon Jo[1,2†], Si Ho Han[3†], Mark Bryan Carayugan[1†], Julia Inacio Carvalho[1], Ye Jin Kong[4], Jong Chan Yeo[1], Lan Thi Ngoc Tran[1], Wencelito Palis Hintural[1,5], S. K. Abidur Rahman[1], Hyun Ju Lee[6], Sang Hyun Park[7], Hyung Won Kim[8], Yu Seon Lee[1], Woo Bin Youn[1], Ji Young An[9*] and Byung Bae Park[1*]

Abstract

Background Understanding the processes underlying carbon storage and balance is critical for equipping the terrestrial biosphere to respond to contemporary climatic challenges. However, ecosystem-level estimates and distribution of net primary productivity (NPP), a metric for evaluating forest carbon cycling patterns and dynamics, remain constrained by uneven empirical observations between above- and belowground fractions. We herein quantified the rate and composition of NPP for four stands characteristic of the cool-temperate deciduous (*Larix kaempferi*, LK; *Quercus mongolica*, QM) and evergreen (*Pinus densiflora*, PD; *Pinus koraiensis*, PK) forests of South Korea over a complete annual cycle (2022–2023). Variations in dynamic NPP compartments, particularly (1) canopy litterfall by stand and season and (2) fine root production by stand, diameter class, and depth interval, were further characterized using litter traps and ingrowth cores, respectively.

Results Total NPP varied from 1226 ± 101 to 1796 ± 154 g m^{-2} yr^{-1}, with 78–84% allocated aboveground and 16–22% belowground. LK and QM exhibited total NPP up to 46% higher than PD and PK. Both litterfall and fine root production differed considerably across stands, decreasing in the order of QM > PK > PD > LK for litterfall and QM & PD > LK & PK for fine root production. Litterfall peaked in autumn, similar to the leaf phenological rhythm of many temperate deciduous species. In contrast, fine root production showed a negative vertical distribution with depth, which is consistent with decreasing nutrient availability and increasing mechanical impedance along the soil profile.

Conclusions By disentangling the contribution levels and dynamic patterns of each NPP compartment, our findings demonstrate a strong inclination toward aboveground NPP investment when belowground resources are not limiting. In other words, an adequate nutrient supply enables plants to modify their priority allocation from fine root maintenance to internal resource transport, leaf production, canopy expansion, reproduction, and other critical

†Min Seon Jo, Si Ho Han, and Mark Bryan Carayugan have contributed equally to this work and share first authorship.

*Correspondence:
Ji Young An
ajy2656@gnu.ac.kr
Byung Bae Park
bbpark@cnu.ac.kr
Full list of author information is available at the end of the article

© The Author(s) 2026. **Open Access** This article is licensed under a Creative Commons Attribution 4.0 International License, which permits use, sharing, adaptation, distribution and reproduction in any medium or format, as long as you give appropriate credit to the original author(s) and the source, provide a link to the Creative Commons licence, and indicate if changes were made. The images or other third party material in this article are included in the article's Creative Commons licence, unless indicated otherwise in a credit line to the material. If material is not included in the article's Creative Commons licence and your intended use is not permitted by statutory regulation or exceeds the permitted use, you will need to obtain permission directly from the copyright holder. To view a copy of this licence, visit http://creativecommons.org/licenses/by/4.0/.

aboveground functions. Such information underscores the necessity for forest management strategies that target soil fertility to strengthen not only canopy productivity and CO_2 sequestration but also ecosystem resilience by reinforcing allocation patterns that sustain high NPP and safeguard forests against shifting climate conditions.

Keywords Biomass increment, Carbon cycle, Fine root production, Litterfall, Net primary production, Temperate forest

Background

Global carbon storage and balance have become a priority theme in ecological research in response to rising atmospheric carbon dioxide (CO_2) concentrations and shifting climate regimes (Anees et al. 2025b; Mehmood et al. 2025a). As forests are responsible for 7.6 billion metric tons of annual CO_2 sequestration and about 45% of organic carbon stored in biomass and soil (Baul et al. 2021; Streiff 2021), a deeper comprehension of their role in the global carbon budget is essential for equipping the terrestrial biosphere to adapt to and address contemporary climatic challenges (Anees et al. 2024, 2025a; Mehmood et al. 2025b). Net primary productivity (NPP), the net immobilization of atmospheric CO_2 into plant biomass, serves as a key indicator of vegetation feedback on climate change (Curiel Yuste et al. 2005). NPP underpins critical forest ecological functions by (1) supplying organic materials to higher trophic levels and (2) modulating climate through carbon and hydrological circulation (Xiao et al. 2003; Agrawal and Gopal 2013). Despite its importance, ecosystem-level estimates of NPP remain limited by observational imbalances among its compartments and persistent methodological uncertainties (Clark et al. 2001; An and Osawa 2021). A recurring challenge in forest NPP research is the tendency to over-rely on aboveground field observations while overlooking belowground counterparts or presupposing their contributions as a fixed, hypothetical fraction of aboveground NPP. In addition, many previous studies contain unreliable estimates of NPP due to weak methodology or insufficient documentation of collection procedures (Clark et al. 2001; An and Osawa 2021). It is therefore fundamental to provide comprehensive, methodologically sound, and empirical measurements of forest NPP compartments to enhance the reliability of ecological assessments, inform local and regional carbon models, and validate carbon flux measurements that contribute not only to maximizing CO_2 sink capacity but also to building forest ecosystem resilience in the face of rapidly changing climate conditions.

Estimating carbon budgets using a bottom-up field approach requires comprehensive quantification of principal NPP components: aboveground biomass accumulation, litterfall, and belowground production (Clark et al. 2001; Malhi et al. 2011). Aboveground biomass encompasses stem and branch biomass increments, which reflect long-term carbon storage investments, canopy leaf area, leaf residence time, photosynthetic capacity, and reproductive structure formation (Malhi et al. 2011). While any live biomass growth in the canopy is accounted for by aboveground increments, a significant portion of leaf material, along with other organs such as twigs, bark fragments, and reproductive structures, is deposited on the ground after senescence as litterfall (Clark et al. 2001; Zhu et al. 2021). Canopy litterfall forms one of the largest NPP compartments, contributing 20–60% of the total annual forest NPP at the landscape scale (Sun et al. 2021; Carayugan et al. 2023). Annual litter flux exhibits a high degree of spatial variability driven by species identity (Jasińska et al. 2020; Zhu et al. 2021) and forest stand structure (Nakagawa et al. 2019; Giweta 2020). Intra-annual litterfall dynamics are also specific to a forest type, ranging from unimodal to bimodal or irregular patterns (Giweta 2020), or may respond to similar environmental cues, such as sudden temperature drops in autumn, moisture deficits during dry season, or heavy rainfall during monsoon season (Carayugan et al. 2023; Lili et al. 2024). Comparative investigation of annual and seasonal litterfall across forest types is therefore necessary to clarify species-specific controls on the timing and quantity of aboveground carbon transfers to soil and atmospheric systems.

The proportion of NPP dedicated to fine roots, potentially amounting to 3–54% of the total annual forest NPP, signals carbon allocation to resource foraging, storage and transport, and soil faunal dynamics (Vogt et al. 1995; Malhi et al. 2011; Fukuzawa et al. 2013). Fine roots exhibit a characteristic vertical structure that can be circumscribed by an exponential model (Ochoa-Hueso et al. 2020). Fine roots typically colonize upper soil layers where the level of mechanical impedance is conducive to expansion and access to nutrients from litterfall is most adequate (Li et al. 2020; Zheng et al. 2024). However, in resource-deficient environments, plants may invest in deeper root growth and maintenance to enhance their foraging capacity and establish a niche in less-exploited sections of the soil profile (Freschet et al. 2018; Li et al. 2020). Besides their unique vertical stratification, fine root populations also consist of a heterogeneous pool

of roots with distinct diameter categories and functions. Thinner diameter classes, located close to the soil interface, predominantly contain roots specialized for water and nutrient capture, whereas thicker diameter classes hold significant amounts of roots functioning in transport and storage (Finér et al. 2007; Liu et al. 2018; Carvalho and Foulkes 2019). Although proven ecologically significant, little is still known about the variations in vertical and diameter-based distribution of fine roots across forest types, primarily due to natural belowground heterogeneity, methodological complexity, and limited reproducibility of observations (Addo-Danso et al. 2016; An and Osawa 2021). Improving empirical understanding of horizon- and size-based root patterns and processes is therefore vital for reducing uncertainties in belowground carbon fluxes and avoiding oversimplified root representations in ecosystem models (Smithwick et al. 2014).

The South Korean side of the East Asian phytogeographic zone supports a unique mosaic of old-growth and secondary forests. Over half of its forested area (i.e., 52%) is composed of temperate deciduous species such as *Quercus mongolica* Fisch. ex Ledeb. and *Larix kaempferi* (Lamb.) Carrière and native evergreen species, including *Pinus densiflora* Siebold & Zucc. and *Pinus koraiensis* Siebold & Zucc. (Carvalho et al. 2025). Their coexistence in a shared geographical and climatic region offers an ideal opportunity to investigate productivity patterns and variations in both aboveground and belowground processes among spatially proximal yet functionally contrasting community types. In this study, we conducted a comprehensive field-based inventory of NPP across four representative cool temperate stands in South Korea. Our main objective was to quantify annual NPP and its allocation for aboveground biomass growth, litterfall, and root production. We also characterized the fraction-specific patterns of annual and seasonal litterfall, as well as the depth- and diameter-based distributions of annual fine root production across different stand types. Our analysis was designed to address the following questions: (1) How is NPP partitioned among aboveground and belowground compartments, and how does this partitioning vary by forest type? (2) What are the magnitudes and intra-annual dynamics of canopy litterfall? (3) Are there distinct diameter and depth classes where fine root production is confined, and do these patterns differ among forest types? By disentangling stand-specific NPP composition, spatiotemporal litterfall patterns, and fine root distribution, this study offers critical insights for advancing regional carbon budgets in temperate forest environments.

Methods

Site description

This study was conducted in Mt. Gariwang, a cool temperate forest located in the inland alpine zone of Gangwon Province, South Korea. The mountain is geographically bound to the west by Mount Jungwang and to the east by Jongseon-eup in Jongseon County and Jinbu-myeon in Pyeongchang County (Jung et al. 2013). Vegetation in Mt. Gariwang is defined by a unique assemblage of natural deciduous forests dominated by *Q. mongolica*, as well as secondary coniferous stands composed of *Pinus* spp., *Abies* spp., and *Taxus* spp. (Jung et al. 2013). The mountain also supports intensively managed plantations of *L. kaempferi*, developed for timber production. The abundant plant community of Mt. Gariwang is an outcome of a balanced implementation of forest protection and sustainable management practices. From 2006 to 2008, approximately 2462 hectares were set aside by the Korea Forest Service (KFS) as protected areas for genetic resource conservation (Lee et al. 2016). A range of sustainable forest management practices is simultaneously implemented in unprotected zones, including forest road network construction, secondary forest and plantation establishment, intermediate cutting operations (e.g., thinning), and reproductive cutting operations (e.g., shelterwood and selective cutting) (Lee et al. 2014).

Mt. Gariwang has a structurally complex geology, consisting of black and gray shale and sandstone dating from the Paleozoic (Ordovician-Permian) to Mesozoic (Triassic) eras (Kim et al. 2025). The dominant soil order is Inceptisols (National Institute of Agricultural Sciences 2025), with textures varying from loam to sandy loam. The regional climatic type is warm-summer humid continental (Köppen classification: Dwb), characterized by hot summers from June to August and long winters from mid-November until early April. Long-term annual temperature (1997–2023) averages 8.7 °C, fluctuating seasonally from a mean of 21 °C in summer to − 5 °C in winter. Total annual precipitation is 1309 mm, with a pronounced seasonality where about three-fifths (60.2%) occurs during the summer monsoon season, and the remaining precipitation is uniformly distributed throughout the rest of the year.

Four stands (37°28′16.14″–37°28′46.31″ N, 128°29′30.68″–128°29′54.13″ E; 934–1048 m asl elevation), each capturing a forest type characteristic of the cool temperate region in South Korea, were selected for a comprehensive measurement of NPP compartments: (1) *L. kaempferi* stand (hereafter, LK), (2) *P. densiflora* stand (hereafter, PD), (3) *P. koraiensis* stand (hereafter, PK), and (4) *Q. mongolica* stand (hereafter, QM) (Fig. 1). These stands feature a unique set of vegetation structural properties, with mean basal area and stand density of ≥ 5 cm

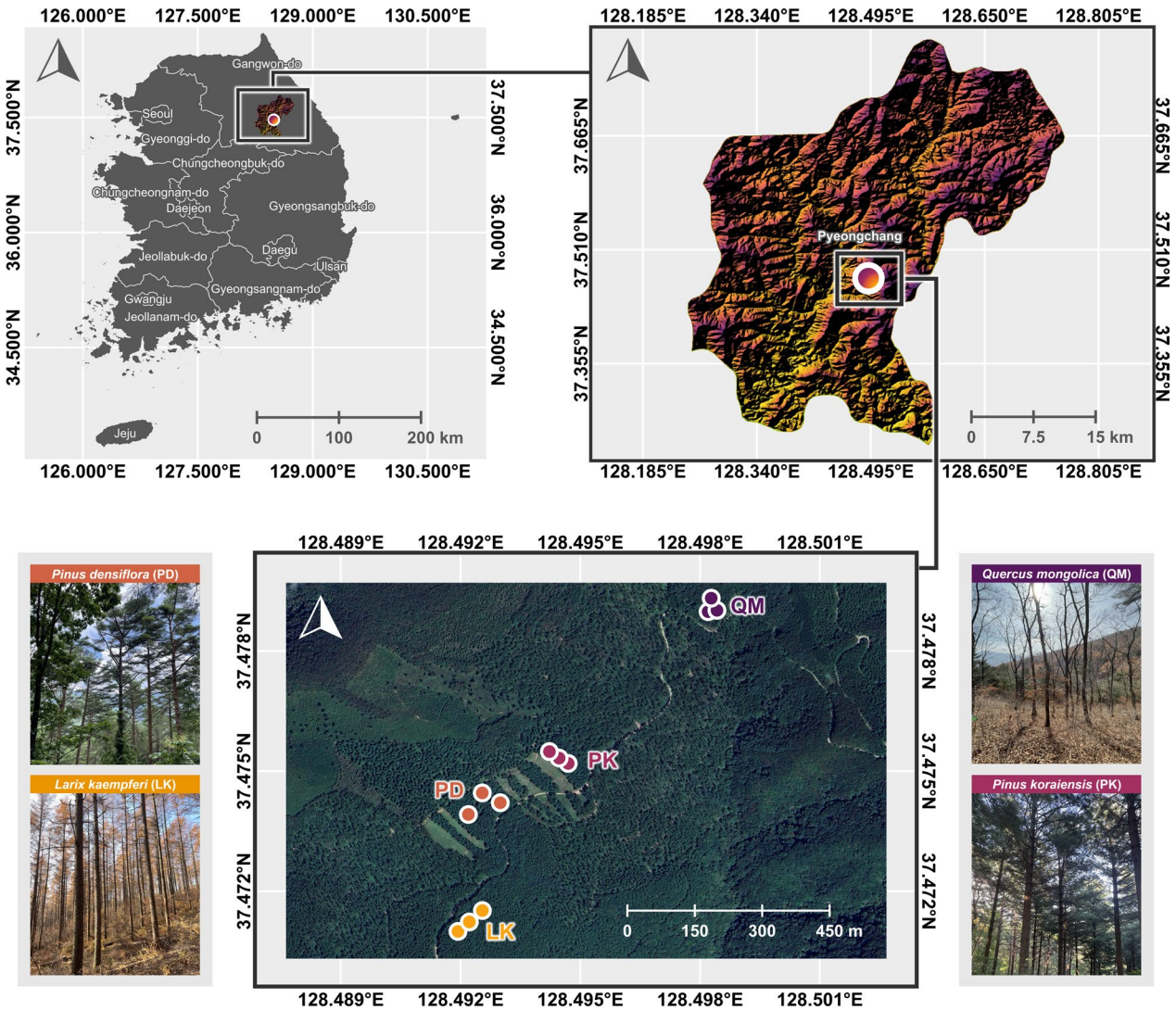


Fig. 1 Geographical location of *Larix kaempferi* (LK), *Pinus densiflora* (PD), *Pinus koraiensis* (PK), and *Quercus mongolica* (QM) stands in Mt. Gariwang, Pyeongchang, Gangwon Province, Republic of Korea

DBH trees ranging from 26.5 to 30.7 m^2 ha^{-1} and 267–758 trees ha^{-1}, respectively (Carvalho et al. 2025). The understory stratum of these stands consists of the following plant species: (1) *Rubus oldhamii* Miq., *Zanthoxylum schinifolium* Siebold & Zucc., *Lindera obtusiloba* Blume, *Tripterygium regelii* Sprague & Takeda, and *Fraxinus rhynchophylla* Hance for LK; (2) *Aralia elata* (Miq.) Seem., *T. regelii*, *R. oldhamii, Z. schinifolium*, and *L. obtusiloba* for PD; (3) *Cornus controversa* Hemsl., *Kalopanax septemlobus* (Thunb.) Koidz., *Styrax obassia* Siebold & Zucc., *F. rhynchophylla,* and *Z. schinifolium* for PK; and (4) *Quercus serrata* Murray, *Acer pseudosieboldianum* (Pax) Kom., *F. rhynchophylla,* and *K. septemlobus* for QM. Edaphic conditions (0–30 cm depth) across stands were generally acidic, with soil pH varying from 4.4 to 5.1 and other soil chemical properties ranging as follows: 8.0–11.9% for soil organic matter (SOM), 0.3 to 0.5% for total nitrogen (TN), 19.6 to 72.1 mg kg^{-1} for available phosphorus (AP), and 5.3 to 10.2 $cmol_c$ kg^{-1} for cation exchange capacity (CEC). A comprehensive summary of the geographic, structural, and edaphic conditions of the investigated stands is presented in Tables S1 and S2.

In August 2022, twelve 400 m^2 plots were systematically established within the selected forest stands, with three replicate plots dedicated to each of the four stand types. A comprehensive vegetation survey was conducted in November 2022 to establish the foundation for allometric biomass estimations and following NPP calculations. All trees with a diameter at breast height (DBH) of at least

5 cm were identified to species level, and their DBH was measured using a diameter tape.

Field-based characterization of NPP

In this study, annual NPP was quantified as the sum of woody biomass increment, litterfall, fine root production, and coarse root biomass increment over a full annual cycle (Van Do et al. 2015). While recognizing that minor NPP losses can occur through herbivory, volatile and leached organics, and root exudation, these components were considered negligible and thus excluded from calculations, following prior studies in forest NPP research (Clark et al. 2001; Malhi et al. 2011). The annual NPP for each investigated stand was expressed using the following equation:

$$\mathrm{NPP} = \Delta\mathrm{WB} + \mathrm{LF} + \mathrm{FRP} + \Delta\mathrm{CRB}$$

where ΔWB is the annual increment in woody biomass (stem and branch), LF is the annual litterfall, FRP is the annual fine root production, and ΔCRB is the annual biomass increment of coarse roots.

Woody biomass increment (ΔWB)

The woody biomass increment (ΔWB) was determined by measuring the DBH of all trees with ≥ 5 cm DBH within each plot. Initial measurements were taken in November 2022 and repeated exactly one year later in November 2023 to capture biomass growth. Individual DBH values were converted to their corresponding stem (W_s) and branch (W_b) biomass estimates using the species-specific allometric equations developed by the National Institute of Forest Science for key temperate species in South Korea (Son et al. 2014) (Table 1).

For each individual tree, WB was calculated by combining the estimated stem and branch biomass components, as in:

$$\mathrm{WB} = \mathrm{W_s} + \mathrm{W_b}$$

Plot-level ΔWB was calculated by combining (1) the change in WB for all trees between 2022 and 2023 and (2) the change in WB of trees that reached the minimum 5 cm diameter threshold during the measurement interval (i.e., ingrowth) (Clark et al. 2001). The resulting values were scaled to units of g m^{-2} yr^{-1}. The ΔWB for each plot was calculated as:

$$\Delta\mathrm{WB} = \sum_{i=1}^{n_{tree}} (WB_{i,2023} - WB_{i,2022}) + \sum_{j=1}^{n_{ingrowth}} (WB_{j,2023} - WB_{j,DBH=5})$$

where $WB_{i,2023}$ and $WB_{i,2022}$ are the woody biomass of a previously measured tree i in 2023 and 2022, respectively; n_{tree} is the total number of previously measured trees; $WB_{j,2023}$ is the total woody biomass of an ingrowth tree j in 2023; $WB_{j,DBH=5}$ is the estimated woody biomass at 5 cm DBH; and $n_{ingrowth}$ is the total number of ingrowth trees.

Table 1 Species-specific allometric equations developed by the National Institute of Forest Science for estimating stem and branch biomass of *Larix kaempferi* (LK), *Pinus densiflora* (PD), *Pinus koraiensis* (PK), and *Quercus mongolica* (QM) in South Korea (Son et al. 2014)

Species	Organ	Equation	R^2
LK	Stem	$W_s = 0.016(DBH)^{2.888}$	0.954
	Branch	$W_b = 0.005(DBH)^{2.774}$	0.633
PD	Stem	$W_s = 0.209(DBH)^{2.087}$	0.960
	Branch	$W_b = 0.069(DBH)^{1.995}$	0.867
PK	Stem	$W_s = 0.064(DBH)^{2.377}$	0.929
	Branch	$W_b = 0.621(DBH)^{1.395}$	0.345
QM	Stem	$W_s = 0.595(DBH)^{1.766}$	0.828
	Branch	$W_b = 0.007(DBH)^{2.970}$	0.845

W_s and W_b indicate dry biomass values of stem and branch in kg, respectively, and DBH is the diameter at breast height in cm. The organ-specific allometric equations were generated from biomass surveys conducted at over 200 locations across South Korea. Each survey location featured a standard 400 m^2 plot where (1) trees with DBH of up to 50 cm for LK, 70 cm for PD, 40 cm for PK, and 40 cm for QM underwent comprehensive inventory, and (2) five standard trees representative of the plot's diameter distribution were harvested for stem and branch dry weight measurement. In target areas with low tree density and trees younger than 20 years, plot dimensions were adjusted to ensure that each plot included at least 10 trees

Canopy litterfall (LF)

A systematic field collection design was implemented from November 2022 to November 2023 to quantify seasonal and annual litterfall. Nine litter traps were stationed within each plot in a 3×3 grid configuration at 5 m spacing intervals, resulting in a total of 27 traps per stand and 108 traps across the entire study. Each trap was mounted directly above the forest floor to intercept free-falling litter with minimal disturbance. The traps featured a 0.29 m^2 circular opening, uniform perforations throughout the collection area for water drainage and air circulation, and a finely meshed netting fabric (119 μm mesh size) tucked securely on all sides of the catchment. The use of such finely sized mesh ensures (1) the retention of minute litterfall components, such as *L. kaempferi* foliage and other fragmented debris (i.e., miscellaneous litter) within the catchment and (2) the effective passage of rainwater through the trap without displacing small litter particles. Litter samples were collected at quarterly intervals corresponding to the following seasons: February 2023 (winter), May 2023 (spring), August 2023 (summer), and November 2023 (autumn). This collection schedule facilitates the

measurement of total litter outputs over a complete annual cycle while allowing for the evaluation of intra-annual pulses in litter activity. Upon collection, litter samples were transported to the laboratory and air-dried to avoid mass losses from decomposition. Litter samples were manually separated into six distinct categories, consisting of two foliar components (dominant and non-dominant leaf) and four non-foliar components (reproductive structure, bark, twig, and miscellaneous debris). Each sorted component was oven-dried at 65 °C for 48 h to a constant mass, then weighed to the nearest 0.1 g using a precision laboratory balance (WBA-6200, Daihan Scientific Co., Ltd., Gangwon-do, Korea). The dry mass of each component was standardized to g m^{-2} to enable analysis of interstand variations in annual and seasonal litterfall and relative NPP allocation to litterfall.

Both ΔWB and LF represent the aboveground compartments of the annual forest NPP, which can be expressed in the following equation:

$$\text{Aboveground NPP} = \Delta\text{WB} + \text{LF}$$

Fine root production (FRP)

Fine root production (FRP) and mortality (FRM) were measured using the ingrowth core method, a widely accepted approach that quantifies root dynamics based on the colonization of a rootless medium by roots from the surrounding soil. Ingrowth coring was selected over other estimation techniques due to its straightforward field application and ease of interpretation (Addo-Danso et al. 2016; An and Osawa 2021). Moreover, this method is suitable for studies comparing fine root demographic processes across various sites and for forests characterized by rapid root growth, aligning well with our research focus and site description (Van Do et al. 2015; An and Osawa 2021). A total of 60 ingrowth core units were installed in November 2022, with 15 units allocated to each of the four target stands and five units allotted per plot. To ensure systematic installation of ingrowth cores per plot, a core unit was buried next to each of the four vertices of the litter trap grid (≤0.1 m from the trap), while one unit was placed near the grid's center. Each core was installed by creating a cylindrical hole measuring 5 cm in diameter and 30 cm in depth using a hollow stainless-steel corer. The excavated soil materials were segregated by horizon based on visual and textural indicators and then sieved to eliminate roots, pebbles, and other debris. A PVC-coated cylinder with a 5 cm diameter opening, 3 mm lateral perforations, and an enmeshed base was mounted into each hole to a depth of 30 cm. These cores were refilled with the sieved soil, stratifying the soil by horizon to simulate the default conditions of a soil monolith. The spaces surrounding the core were backfilled with the remaining root-free soil to ensure a snug fit. The cores were left in situ from November 2022 to November 2023 to allow a full year of root recolonization. In November 2023, all ingrowth cores were retrieved from the ground, sealed in plastic bags, and refrigerated at − 2 °C until processing. In the laboratory, each sample was vertically stratified into 5 cm depth increments: 0–5 cm, 5–10 cm, 10–15 cm, 15–20 cm, 20–25 cm, and 25–30 cm, and fine roots were manually extracted from each depth class through manual picking and sieving. Extracted root samples were washed thoroughly with water until all adhering soil particles were removed. Extracted roots were then classified into diameter classes of < 0.5 mm, 0.5–1 mm, and 1–2 mm. This diameter-based classification was adopted due to its ability to reflect multiple physiological and chemical traits that support root development, as well as its operational efficiency in processing large-scale root cohorts or fragments relative to root order, an especially valuable classification for evaluating specific patterns of root segments (e.g., elongation and penetration) (Liu et al. 2018; Zhuang et al. 2018; Freschet et al. 2018). Following diameter stratification, each root sample was further sorted into live and dead fractions based on the visual indicators described by Tran et al. (2024). Live roots are distinguished by their degree of flexibility when bent and a pale to light brown exterior. In contrast, roots were designated as dead if they exhibited darker coloration, brittleness, and a tendency to break when bent (Tran et al. 2024). All sorted root samples were oven-dried at 65 °C for 48 h to constant weight, weighed to the nearest 0.1 g, and expressed in g m^{-2} yr^{-1} units to allow quantitative comparison by depth, diameter class, and stand type.

Annual FRP and FRM were derived by balancing estimates of living and dead root stocks using the decision matrix simplified by Yuan and Chen (2013) from Fairley and Alexander (1985) (Table 2). This matrix estimates FRP and FRM based on changes in living and dead root mass during a measurement interval, providing a mathematical logic that facilitates calculations across large datasets (An and Osawa 2021). This approach is particularly suitable in contexts where (1) information on litterbag-based mass loss rate is unavailable and (2) alternative estimation techniques, such as continuous inflow or bootstrap methods, yield a high proportion of negative values for production and mortality (Van Do et al. 2015; An and Osawa 2021). Considering that the ingrowth cores were initially installed under root-free conditions in November 2022, only the first option of the decision matrix (i.e., ΔLF + ΔDF for FRP and ΔDF for FRM) was used to rationalize the annual FRP and FRM.

Biomass increment of coarse roots (ΔCRB)

The annual increment of coarse root biomass (ΔCRB) was calculated by converting the same DBH values used

Table 2 Simplified decision matrix (Yuan and Chen 2013) for estimating fine root production and mortality at the four investigated stands in Mt. Gariwang, Gangwon Province, South Korea

Option	Production	Mortality
$\Delta LF + \Delta DF \geq 0$ and $\Delta DF \geq 0$	ΔLF+ΔDF	ΔDF
$\Delta LF \geq 0$ and $\Delta DF \leq 0$	ΔLF	0
$\Delta LF \leq 0$ and $\Delta LF + \Delta DF \leq 0$	0	|ΔLF|

Δ indicates the change in the mass of live fine root stock (LF) and dead fine root stock (DF)

Table 3 Species-specific allometric equations developed by the National Institute of Forest Science for estimating coarse root biomass of *Larix kaempferi* (LK), *Pinus densiflora* (PD), *Pinus koraiensis* (PK), and *Quercus mongolica* (QM) in South Korea (Son et al. 2014)

Species	Equation	R^2
LK	$CRB = 0.009(DBH)^{2.806}$	0.796
PD	$CRB = 0.231(DBH)^{1.753}$	0.875
PK	$CRB = 0.056(DBH)^{2.175}$	0.903
QM	$CRB = 0.691(DBH)^{1.526}$	0.711

CRB signifies dry biomass values of coarse roots in kg, and DBH is the diameter at breast height in cm. The organ-specific allometric equations were generated from biomass surveys conducted at over 200 locations across South Korea. Each survey location featured a standard 400 m^2 plot where (1) trees with DBH of up to 50 cm for LK, 70 cm for PD, 40 cm for PK, and 40 cm for QM underwent comprehensive inventory, and (2) structural root systems of two standard trees (i.e., the 2nd and 4th of the five standard trees for woody biomass sampling) were excavated to measure coarse root dry weight. In target areas with low tree density and trees younger than 20 years, plot dimensions were adjusted to ensure that each plot included at least 10 trees

for woody biomass estimations into their corresponding coarse root biomass equivalents. The species-specific equations used for estimating coarse root biomass, obtained from the National Institute of Forest Science (Son et al. 2014), are summarized in Table 3.

ΔCRB was calculated for each plot by subtracting the increment in CRB for both previously measured and ingrowth trees between 2022 and 2023. The subsequent values were then scaled to units of g m^{-2} yr^{-1}. Plot-level ΔCRB was determined through the following equation:

$$\Delta CRB = \sum_{i=1}^{n_{tree}} (CRB_{i,2023} - CRB_{i,2022}) + \sum_{j=1}^{n_{ingrowth}} \left(CRB_{j,2023} - CRB_{j,DBH=5}\right)$$

where $CRB_{i,2023}$ and $CRB_{i,2022}$ represent the coarse root biomass of a previously measured tree i in 2023 and 2022, respectively; n_{tree} is the total number of previously measured trees; $CRB_{j,2023}$ is the coarse root biomass of an ingrowth tree j in 2023; $CRB_{j,DBH=5}$ is the estimated coarse root biomass at 5 cm DBH; and $n_{ingrowth}$ is the total number of ingrowth trees between 2022 and 2023.

FRP and ΔCRB estimates were combined to determine the plot-level annual belowground NPP at each of the four stands, as in:

$$\text{Belowground NPP} = \text{FRP} + \Delta CRB$$

Data analysis

All datasets were assessed for residual normality via the Shapiro–Wilk test and for homogeneity of variance via Levene's test to ensure that the characterization of NPP and its compartments met the assumptions required for parametric mean comparisons. Datasets that did not meet the necessary conditions were subjected to logarithmic transformation prior to the parametric test proper. A comparative analysis of total NPP, total litterfall, and component-specific litterfall across stands was performed using one-way analysis of variance (ANOVA), with plots serving as replicates. Three-way ANOVA was employed to test for the interactive effects of stand, soil depth, and fine root diameter class on FRP and FRM. In cases where three-way interactions were insignificant, two-way ANOVA was applied to evaluate all possible second-order interactions (e.g., Stand × Depth, Stand × Diameter, Depth × Diameter), followed by one-way ANOVA to isolate the effects of individual factors. All significantly different group means were classified into their respective homogeneous subsets using Duncan's Multiple Range Test, which controls for multiple comparisons through p-value adjustments. All statistical analyses were performed using SPSS Statistics for Windows ver. 26.0 (SPSS Inc., Chicago, IL), with significance thresholds set at $p < 0.05$.

Results

Annual NPP rate and compartmental allocation

Annual total NPP exhibited significant inter-stand variation, ranging from 1226 ± 101 to 1796 ± 154 g m^{-2} yr^{-1} (Fig. 2). LK and QM had the highest total annual NPP, surpassing that of PD by up to 13% and PK by as much as 46% ($F = 4.5$; $p < 0.05$). Aboveground components formed the dominant share of total NPP at 78–84% across stands. Total belowground NPP, on the other hand, accounted for a smaller but considerable proportion at 16–22% (198 ± 38 to 385 ± 39 g m^{-2} yr^{-1}). Within the belowground

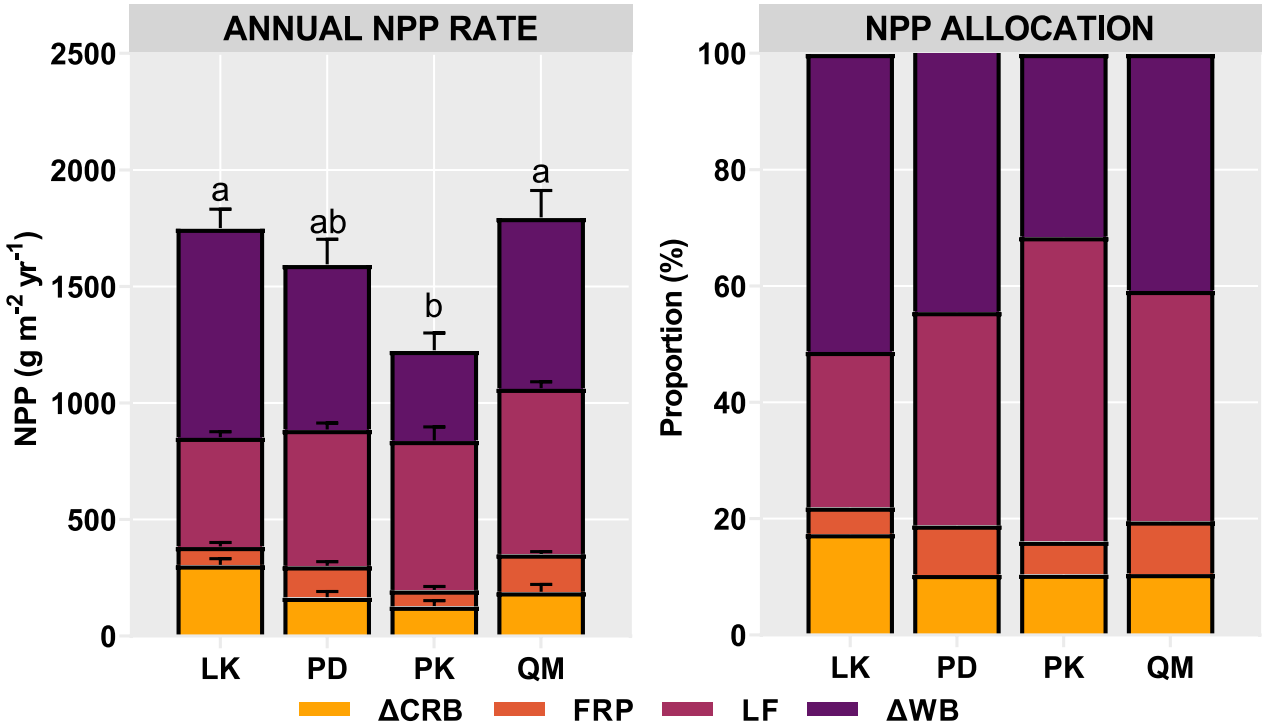


Fig. 2 Annual rate (g m^{-2} yr^{-1}) and percent contribution (%) of woody biomass increment (ΔWB), litterfall (LF), fine root production (FRP), and coarse root biomass increment (ΔCRB) to the net primary productivity (NPP) of *Larix kaempferi* (LK), *Pinus densiflora* (PD), *Pinus koraiensis* (PK), and *Quercus mongolica* (QM) stands in Mt. Gariwang, Pyeongchang, Gangwon Province, Republic of Korea. Vertical bars indicate the standard error of the mean ($n = 3$). Different lowercase letters signify significant differences among stands, as determined by Duncan's Multiple Range Test ($p < 0.05$)

compartment, FRP accounted for a smaller proportion of the belowground production compared to ΔCRB, with values of 21% for LK, 45% for PD, 35% for PK, and 46% for QM.

Variation patterns of canopy litterfall

Total and component-specific litterfall showed significant variation across stands, with the exception of twig ($F = 3.7$; $p = 0.060$) and miscellaneous litter ($F = 1.0$; $p = 0.443$), which remained consistent within a range of 35 ± 0.4 to 99 ± 6 g m^{-2} yr^{-1} and 13 ± 2 to 65 ± 49 g m^{-2} yr^{-1}, respectively (Table S3). Annual total litterfall was found to be highest in QM and PK (711 ± 27 g m^{-2} yr^{-1} for QM and 642 ± 58 g m^{-2} yr^{-1} for PK), exceeding that of PD by 10–22% and LK by 37–52% ($F = 7.8$; $p < 0.01$, Fig. 3). Dominant leaf litterfall was comparable among QM and PK but significantly lower in LK and PD, where their annual production averaged 293 ± 8 g m^{-2} yr^{-1} and 218 ± 27 g m^{-2} yr^{-1}, respectively ($F = 12.6$; $p < 0.01$). PD and QM recorded the highest non-dominant leaf litterfall at 157 ± 23 g m^{-2} yr^{-1} for PD and 131 ± 13 g m^{-2} yr^{-1} for QM, followed by PK (44 ± 20 g m^{-2} yr^{-1}) and LK (43 ± 14 g m^{-2} yr^{-1}) ($F = 10.9$; $p < 0.01$). Annual reproductive litter was highest in PK, intermediate in QM and PD, and lowest in LK ($F = 50.5$; $p < 0.001$), while bark litter was highest in PD, intermediate in PK and QM, and lowest in LK ($F = 12.7$; $p < 0.01$).

Leaves from both dominant and non-dominant species collectively formed the majority of litterfall, ranging from 63 to 72%. The compositional pattern of litterfall was distinct for each stand, conforming to the following decreasing order of contribution: (1) leaf > twig > bark > miscellaneous > reproductive for LK, (2) leaf > twig and bark > reproductive > miscellaneous for PD, (3) leaf > reproductive > miscellaneous > bark > twig for PK, and (4) leaf > twig > reproductive > bark > miscellaneous for QM.

All four stands experienced an autumnal total litterfall peak, with 52% of their annual litterfall occurring between September and November (Fig. 4). Senescent leaves from both dominant and non-dominant species consistently peaked during autumn across all stands, with some leaf deposition extending into early winter (e.g., 80 ± 18 g m^{-2} of dominant leaf in PD and 57 ± 5 g m^{-2} of non-dominant leaf in QM; Table S4). Over 83% of annual reproductive litter in PK and PD was deposited from summer through autumn (40 ± 3 to 85 ± 9 g m^{-2}), while peak reproductive input in QM occurred exclusively in autumn (23 ± 5 g m^{-2}). In

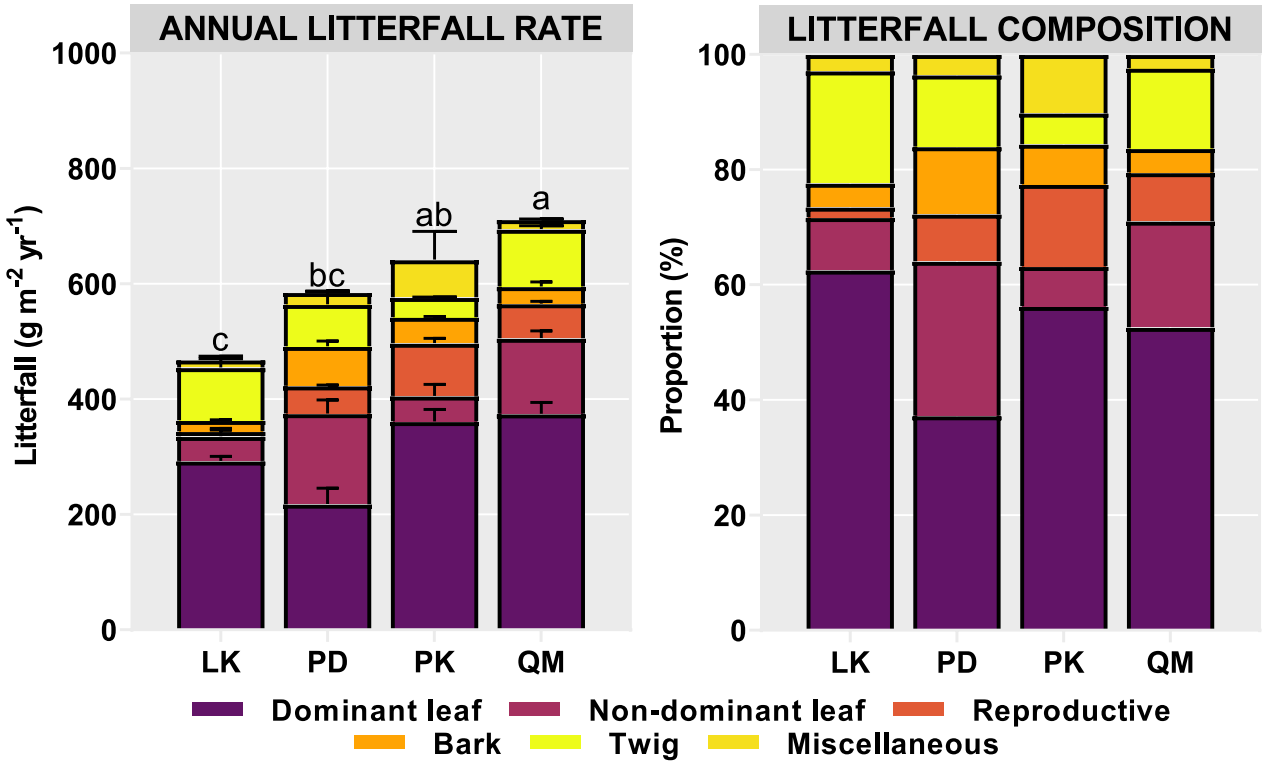


Fig. 3 Annual rate (g m^{-2} yr^{-1}) and percent contribution (%) of dominant leaf, non-dominant leaf, reproductive structure, bark, twig, and miscellaneous debris to the total litterfall pool in *Larix kaempferi* (LK), *Pinus densiflora* (PD), *Pinus koraiensis* (PK), and *Quercus mongolica* (QM) stands of Mt. Gariwang, Pyeongchang, Gangwon Province, Republic of Korea. Vertical bars represent the standard error of the mean ($n = 3$). Different lowercase letters indicate significant differences among stands, as determined by Duncan's Multiple Range Test ($p < 0.05$). Dominant leaf refers to the abscised foliar organs of *L. kaempferi, P. densiflora, P. koraiensis,* and *Q. mongolica* for LK, PD, PK, and QM stands, respectively. Non-dominant leaf refers to leaves from species other than the dominant ones

contrast, LK did not exhibit any discernible pattern in reproductive litterfall.

Bark litterfall demonstrated heterogeneous seasonal highs across stands. PD and PK recorded maximum bark inputs in summer (17 ± 3 to 24 ± 5 g m^{-2}), while LK and QM showed peak bark litterfall during winter (7 ± 1 g m^{-2} for LK, 14 ± 2 g m^{-2} for QM). Twig litterfall exhibited a sharp vernal peak in LK at 59 ± 11 g m^{-2}, and a pronounced autumnal peak in PD at 40 ± 16 g m^{-2}. In the remaining stands, twig litterfall appeared relatively evenly distributed across seasons, except during winter for PK and in spring for QM. Finally, miscellaneous litterfall peaked asynchronously across sites: spring in PK (53 ± 49 g m^{-2}), spring to summer in LK (10 ± 1 g m^{-2}), autumn in PD (10 ± 2 g m^{-2}), and winter in QM (11 ± 0.1 g m^{-2}).

Variation patterns of FRP

Annual total FRP in the upper 30 cm of the soil profile ranged from 69 ± 15 to 162 ± 10 g m^{-2} yr^{-1}, decreasing across stands in the order of QM & PD > LK & PK ($F = 8.8$; $p < 0.01$; Table 4). Fine roots < 0.5 mm in diameter accounted for 58–81% of the total FRP across all stands, mirroring the observed inter-stand variations in overall FRP ($F = 8.5$; $p < 0.01$). Production of roots in the 0.5–1 mm diameter class maintained a stable rate of 11 ± 4 to 32 ± 2 g m^{-2} yr^{-1} ($F = 3.3$; $p = 0.08$), while those in the 1–2 mm diameter class showed a more pronounced inter-stand variation, with QM exhibiting the highest annual production rate at 24 ± 3 g m^{-2} yr^{-1} ($F = 6.3$; $p < 0.05$). Recolonization of 0.5–1 mm and 1–2 mm roots within ingrowth cores contributed 13–25% and 7–17% to the annual FRP, respectively. Annual FRM remained consistent across stands, with total annual rates of 1 ± 0.6 g m^{-2} yr^{-1} for QM and LK, 4 ± 2 g m^{-2} yr^{-1} for PK, and 10 ± 6 g m^{-2} yr^{-1} for PD ($F = 2.1$; $p = 0.18$). Diameter-based partitioning of FRM revealed a high contribution of < 0.5 mm roots to annual FRM (64%), followed by 0.5–1 mm roots (27%) and 1–2 mm roots (9%).

FRP showed a consistently decreasing pattern with increasing soil depth. However, the depth thresholds at

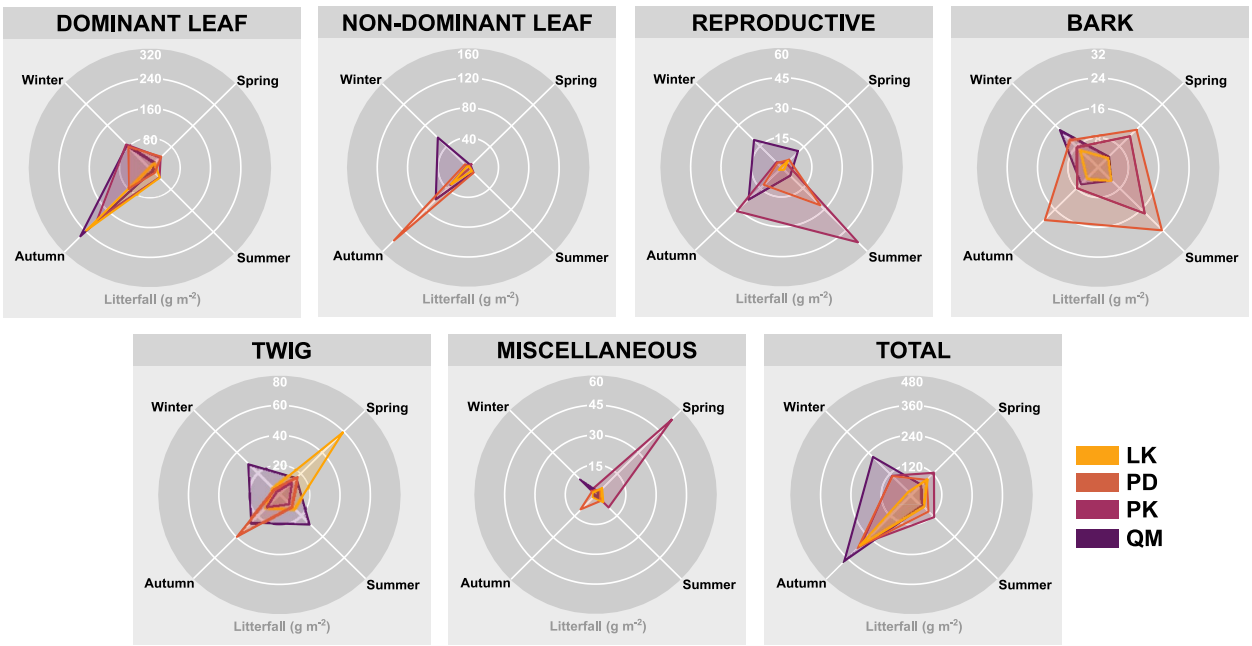


Fig. 4 Seasonal dynamics of dominant leaf, non-dominant leaf, reproductive, bark, twig, miscellaneous, and total litterfall in *Larix kaempferi* (LK), *Pinus densiflora* (PD), *Pinus koraiensis* (PK), and *Quercus mongolica* (QM) stands of Mt. Gariwang, Pyeongchang, Gangwon Province, Republic of Korea. Dominant leaf refers to the abscised foliar organs of *L. kaempferi*, *P. densiflora*, *P. koraiensis*, and *Q. mongolica* for LK, PD, PK, and QM stands, respectively. Non-dominant leaf refers to leaves from species other than the dominant ones

Table 4 Annual production and mortality (g m^{-2} yr^{-1}) of < 0.5 mm, 0.5–1 mm, 1–2 mm, and < 2 mm (total) roots in *Larix kaempferi* (LK), *Pinus densiflora* (PD), *Pinus koraiensis* (PK), and *Quercus mongolica* (QM) stands of Mt. Gariwang, Pyeongchang, Gangwon Province, Republic of Korea, along with a summary of one-way ANOVA describing the effect of stand type on fine root demographics

Stand	FRP (g m^{-2} yr^{-1})				FRM (g m^{-2} yr^{-1})			
	< 0.5 mm	**0.5–1 mm**	**1–2 mm**	**< 2 mm**	**< 0.5 mm**	**0.5–1 mm**	**1–2 mm**	**< 2 mm**
Fine root demographics								
LK	64.6 (13.1)^{b}	10.8 (3.8)^{a}	4.6 (2.3)^{b}	80.0 (16)^{b}	0.6 (0.6)^{a}	0.2 (0.2)^{a}	0.1 (0.1)^{a}	0.8 (0.8)^{a}
PD	108.3 (16.1)^{a}	17.2 (4.3)^{a}	9.6 (1.9)^{b}	135.2 (18.2)^{a}	5.8 (5.1)^{a}	2.8 (1.6)^{a}	1.3 (0.7)^{a}	10.0 (5.6)^{a}
PK	40.1 (1.6)^{b}	17.3 (7.9)^{a}	12 (5.4)^{b}	69.4 (14.6)^{b}	2.5 (1.4)^{a}	0.8 (0.6)^{a}	0.4 (0.4)^{a}	3.6 (1.8)^{a}
QM	106.1 (9.3)^{a}	31.9 (1.8)^{a}	24.3 (2.5)^{a}	162.3 (9.7)^{a}	0.4 (0.2)^{a}	0.3 (0.1)^{a}	0.0 (0.0)^{a}	0.7 (0.4)^{a}
ANOVA (Variation source: Stand)								
F-value	8.494	3.299	6.246	8.802	0.899	2.104	2.034	2.105
p	**< 0.01**	0.079	**< 0.05**	**< 0.01**	0.483	0.178	0.188	0.178

Values enclosed in parentheses indicate the standard error of the mean ($n = 3$). Different lowercase superscripts within a column indicate significant inter-stand variation in FRP or FRM for a given root diameter category, based on Duncan's Multiple Range Test ($p < 0.05$)

which FRP was concentrated ($F = 2.5$; $p < 0.01$; Table S5), as well as the fine root diameter classes contributing most strongly to vertical heterogeneity, were specific to each stand ($F = 12.8$; $p < 0.001$). The production of < 2 mm roots significantly declined with depth in LK, PD, and QM. Notably, FRP maxima (< 2 mm) were found within the uppermost 5 cm in LK, 10 cm in QM, and 15 cm in PD, with these layers capturing 38, 46, and 66% of the total annual FRP for each stand, respectively (Fig. 5). A similar negative vertical distribution was observed for roots < 0.5 mm in LK, PD, and QM, and for 0.5–1 mm roots in LK and QM. In contrast, the production of 1–2 mm roots remained relatively consistent across depths in most stands, except in QM, where 84% of FRP was confined to the 5–20 cm soil depth, with the remaining production evenly distributed across other depth intervals (Table S6). In the case of PK, only < 0.5 mm roots exhibited a significant decrease in FRP with depth,

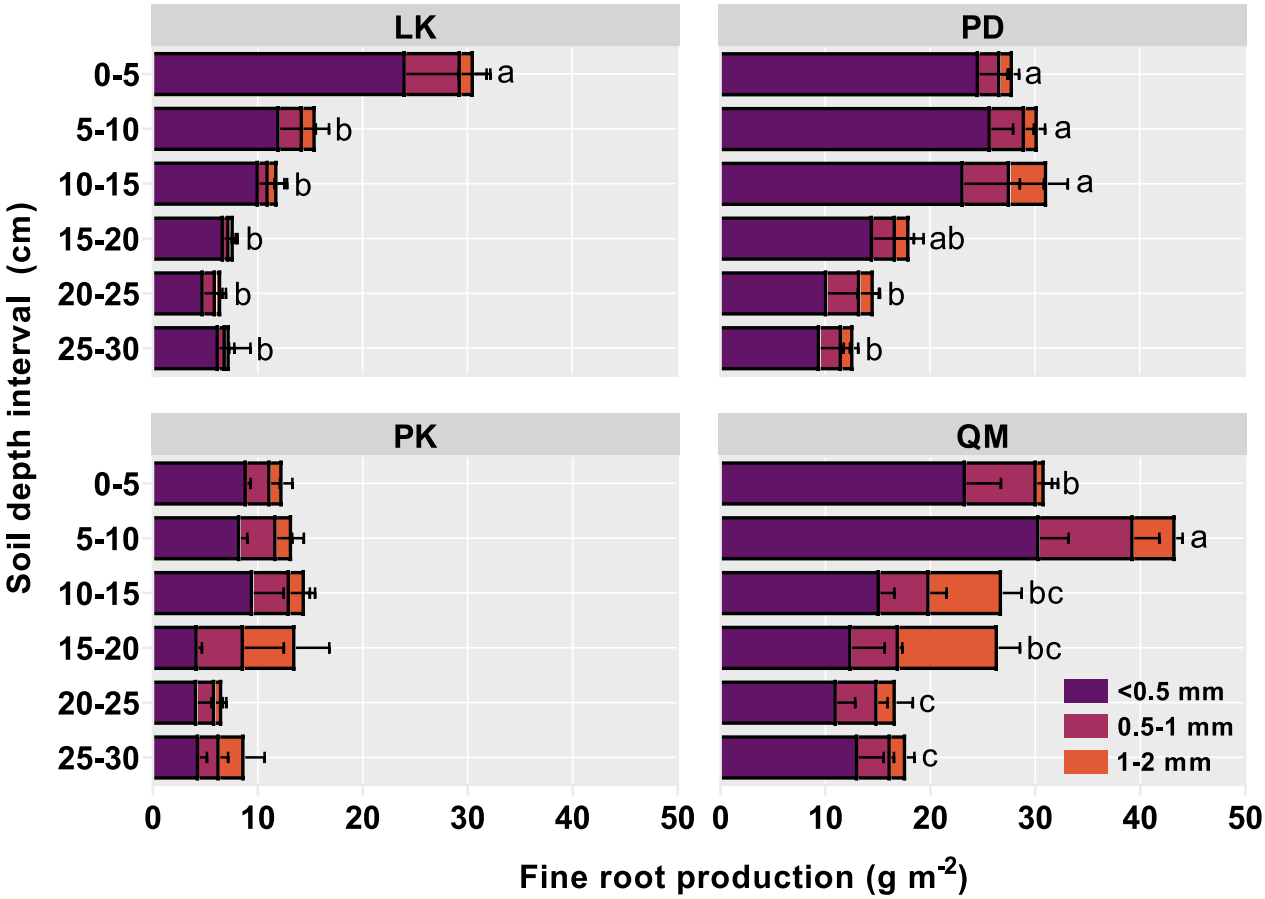


Fig. 5 Depth-wise distribution of fine root production (g m^{-2}) among < 0.5 mm, 0.5–1 mm, and 1–2 mm-sized roots in *Larix kaempferi* (LK), *Pinus densiflora* (PD), *Pinus koraiensis* (PK), and *Quercus mongolica* (QM) stands of Mt. Gariwang, Pyeongchang, Gangwon Province, Republic of Korea. Horizontal bars represent the standard error of the mean ($n = 3$). Contrasting lowercase letters indicate significant differences in total FRP (< 2 mm roots) across depths, as determined by Duncan's Multiple Range Test ($p < 0.05$)

while thicker size classes and total fine roots (< 2 mm) showed no pronounced variation with depth. Notably, the upper 15 cm of the soil profile in PK supported 67% of the production of < 0.5 mm roots. As for FRM, both total and diameter-specific mortality rates were uniform across depth in all four stands ($F = 1.0$; $p = 0.47$; Table S7).

Discussion

Interspecific variation and proportional distribution of NPP

The annual total NPP in this study ranged from 1226 ± 101 to 1796 ± 154 g m^{-2} yr^{-1}, partially aligning with previous estimates for temperate deciduous forests (880–1,410 g m^{-2} yr^{-1}, Tateno et al. 2004), while broadly overlapping with the 1,696 g m^{-2} yr^{-1} reported for a temperate evergreen forest (Van Do et al. 2015). Among the investigated stands, LK and QM exhibited the highest total NPP, surpassing PD and PK by as much as 46%. This pattern is consistent with earlier comparative studies that documented higher NPP outputs for deciduous vegetation relative to their evergreen counterparts (e.g., Mngadi et al. 2022; Tang et al. 2010). The greater productivity of deciduous stands can be attributed to several physiological advantages, such as high light interception capacity and rapid conversion of photosynthetically active radiation to dry matter (Gower et al. 1997; Joshi et al. 2024). A direct proportional relationship has been established between aboveground NPP and leaf area index, with such an association being pronounced in stands dominated by deciduous species (Behera et al. 2015; Singh et al. 2019). Although evergreens engage in continuous carbon assimilation throughout the year, their photosynthetic output during the dormant season is often insufficient to compensate for the LAI advantage and the superior growth-season photosynthetic performance of deciduous species (Curiel Yuste et al. 2005; Baldocchi et al. 2010). Moreover, deciduous species face fewer constraints on carbon allocation to roots and belowground symbionts, further contributing to their

productivity advantage (Tomlinson et al. 2013; Xie et al. 2024). These pronounced productivity variations underscore the necessity of differentiating deciduous and evergreen forests in terrestrial NPP models, suggesting the adoption of allocation coefficients that consider the fundamental distinctions between the two functional types. Besides analysis by plant functional type, interstand assessments of total and compartment-based NPP must thoroughly examine the impacts of both stand age and forest management, as carbon allocation patterns and species-specific growth strategies can vary with developmental stage, leading to differences in NPP among forest types (Zhou et al. 2019). Furthermore, since forest management alters vegetation composition, structure, and resource use, evaluating these practices helps disentangle management-related changes in NPP from those driven by biotic and abiotic factors (Zhang et al. 2020).

The proportional allocation of NPP to aboveground and belowground components remained broadly consistent across all four stands. On average, aboveground compartments formed the majority of the total annual NPP, occupying 78–84%, while belowground compartments constituted a smaller proportion, ranging from 16 to 22%. This distribution pattern falls slightly outside the typical ranges observed in resource-limited environments, where belowground investment tends to be proportionally greater (Wright et al. 2011; Doughty et al. 2018), but aligns well with observations in forests characterized by moderate to high resource availability (Keyes and Grier 1981; Ostonen et al. 2005). The sink-source theory provides a reasonable explanation for these observed allocation patterns, positing that plants modify their carbon distribution between aboveground and belowground structures depending on resource availability (Aragão et al. 2009). Under nutrient-poor conditions, plants often invest more heavily in fine root production to enhance nutrient acquisition, often at the cost of stem, branch, and other aboveground structural growth (Wright et al. 2011; Wurzburger and Wright 2015). In contrast, adequate nutrient availability reduces the need for plants to prioritize photosynthate allocation to fine root maintenance (Xiao et al. 2003; Wurzburger and Wright 2015). In the present study, all stands exhibited sufficient levels of soil organic matter (8.0–11.9%) and nutrient concentrations (total N: 0.3–0.5%; available P: 19.6–72.1 mg kg^{-1}; exchangeable cations: 5.3–10.2 $cmol_c$ kg^{-1}). Considering these relatively favorable and uniform resource conditions, it is possible that the dominant vegetation was relieved of the need for extensive root development to exploit a larger soil surface area. This likely enabled them to channel significant resource investments into critical aboveground functions, such as internal water and nutrient distribution, long-term carbon storage, leaf production, canopy expansion, photosynthesis, and the formation of reproductive structures like flowers and fruits (Malhi et al. 2011).

Annual and seasonal litterfall dynamics

Our investigations into total annual litterfall across stands reveal quantities similar to those of other Korean forests (e.g., 300–656 g m^{-2} yr^{-1}, An et al. 2017; 395–548 g m^{-2} yr^{-1}, Jeong et al. 2009) and other temperate forest zones worldwide (e.g., 470–600 g m^{-2} yr^{-1}, Zhang et al. 2014; 367–486 g m^{-2} yr^{-1}, Zhou et al. 2014). The composition of litterfall reflects a complex interplay of various exogenous and endogenous factors that vary with stand type and dominant species composition (Zhu et al. 2021). Consistent with prior studies, senescent leaves from both dominant and non-dominant species constituted the largest fraction of total litterfall in all four stands, underscoring the role of leaf litter in regulating the overall quantity, physicochemical characteristics, and seasonality of organic matter inputs to the forest floor (Zhu et al. 2021; Lili et al. 2024). The composition of non-foliar litter components showed stand-specific variations, with (1) high twig litter deposits observed in LK, PD, and QM; (2) bark in PD; and (3) reproductive structure in PK. The substantial proportion of twig litter in LK, PD, and QM possibly reflects an active self-pruning mechanism that precedes the development of new twigs during the growing season. The high quantity of bark litter in PD, relative to other non-foliar fractions, is likely related to species-specific traits such as the characteristic bark exfoliation of *P. densiflora* (Jeong et al. 2009). Meanwhile, the proliferation of reproductive litter in PK may have been influenced by *P. koraiensis*' preferential investment in offspring production past the early stages of tree development, similar to those observed in a mixed *P. koraiensis* forest in northeastern China (Wang et al. 2021). These unique patterns in litter composition across stands are indicative of vegetation-specific strategies for aboveground growth allocation, where species modify the relative distribution of their canopy organs to ensure maximum utilization efficiency of available growing space and resources (Lili et al. 2024).

Litterfall exhibits distinct intra-annual pulses that closely mirror the physiological response of plants to seasonal climatic fluctuations (Zhang et al. 2014; Giweta 2020). A clear unimodal trend was observed across all investigated stands, synchronizing with the phenological cycles of many temperate species (Carayugan et al. 2023). Total litterfall production was especially high during autumn as deciduous species increased the production of abscission-inducing hormones to promote leaf drop. This process facilitates two critical functions: (1) internal nutrient transfers from acquisitive to storage plant organs

and (2) directing energy investments toward winter survival (Helmisaari 1992; Wang et al. 2021). While many evergreens continuously manufacture new foliar organs in spring and discard older ones throughout the year, these species can also undergo increased foliar shedding in autumn as a stress response to abrupt climatic shifts (Jeong et al. 2009).

Reproductive litterfall was concentrated between summer and autumn, reflecting the reproductive phenology of the investigated *Pinus* and *Quercus* species. *P. densiflora* is known to abort up to 90% of its seeds and seed cones during summer, especially under dry conditions and when fertilization rates are low (Kang 1999, 2005). *P. koraiensis* exhibits significant cone enlargement in early summer, with seed maturation and dispersal occurring from late summer through early autumn (Song et al. 2023; Zhao et al. 2025). Species whose seeds are primarily dispersed by animals, such as *Q. mongolica*, also experience seed rains throughout autumn, transferring substantial amounts of seed litter materials from the canopy to the forest floor (Wang et al. 2021). In contrast to the relatively predictable patterns of foliar and reproductive litterfall, fine woody litter, such as twigs and bark fragments, demonstrated greater fine-scale temporal variation across stands, likely reflecting a combination of long canopy residence time, temporally uncertain organ turnover, and sensitivity to both current and antecedent environmental conditions (Sun et al. 2021; Carayugan et al. 2025). These characteristics complicate the intra-annual prediction of litterfall, highlighting the need for observations with longer temporal resolution to fully capture their dynamics and contributions to forest floor inputs.

Annual rate and variation pattern of FRP

Our annual FRP values, ranging from 69 ± 15 to 162 ± 10 g m^{-2} yr^{-1}, partly align with estimates reported for secondary forests dominated by *Chamaecyparis obtusa* (Siebold & Zucc.) Endl. and *Quercus serrata* Roxb. (90–159 g m^{-2} yr^{-1}; An and Osawa 2021), but are notably lower compared to other cool temperate broadleaf and conifer forests located in the same region (589–726 g m^{-2} yr^{-1}, Fukuzawa et al. 2013; 360 g m^{-2} yr^{-1}, Tateno et al. 2004). The consistently low FRP observed in all stands mirrors the condition-dependent NPP partitioning strategy of plants, where investment in fine roots is reduced in the absence of soil nutrient limitation (Wright et al. 2011; Wurzburger and Wright 2015).

Pronounced variations in annual FRP were noted among the four investigated stands. Although abiotic factors such as soil nutrient availability and microclimate can influence FRP, the interplay of these conditioning environmental factors was likely overshadowed by dominant species identity (Li et al. 2020). Tree species, in particular, exhibit unique patterns of carbohydrate allocation and supply for root growth, which can significantly impact FRP (Quan et al. 2010; Epron et al. 2011). Across all stands, roots with diameters < 0.5 mm consistently accounted for more than half of the total FRP. Thinner roots are known to exhibit higher resource absorption and metabolic rates (e.g., respiration) relative to thicker roots. Considering an adequate supply of photosynthates, plants prioritize the production of thinner roots to enhance their capacity for nutrient and moisture foraging from the soil (Eissenstat and Yanai 1997).

High FRP was observed in the shallow soil horizons, particularly within the upper 5 cm for < 2 mm roots in LK, the upper 10 cm for < 2 mm roots in QM, and the upper 15 cm for both < 0.5 mm roots in PK and < 2 mm roots in PD. This general pattern of decreasing FRP with soil depth is consistent with the typical negative distribution of nutrients along the soil profile (Quan et al. 2010; Li et al. 2020; Zheng et al. 2024). Confining FRP to shallow layers enables plants to efficiently capture nutrients as they are mineralized from litterfall or released from decomposing organic matter through mycorrhizal interactions or the exudation of extracellular compounds (Cordeiro et al. 2020; Zheng et al. 2024). Many of the roots proliferating in the soil surface layer belong to the thinnest size classes, allowing them to ramify into larger soil volumes and absorb nutrients without allocating as much carbon to biomass and structural development (Cordeiro et al. 2020). This mechanism potentially explains the sharp vertical decline of < 0.5 mm roots in all stands, but not for higher diameter classes (i.e., 0.5–2 mm for PD and PK and 1–2 mm for LK and QM). Furthermore, differences in bulk density may have contributed to the distinct vertical patterns of FRP. High soil bulk density in deeper layers can impose mechanical impedance to root penetration, particularly for thin roots, thereby constraining their downward proliferation and reinforcing their distribution in the upper soil profile (Li et al. 2020; Zheng et al. 2024).

Limitations of the present study

Our collected belowground FRP and FRM data, while demonstrating the value of accurate vertical profiling of diameter-specific fine root distributions, were constrained by a lack of seasonally partitioned observations. Seasonal shifts in surface temperature and rainfall normally regulate soil temperature, moisture, and nutrients that are crucial for plants' internal investment in belowground activity (Quan et al. 2010; An and Osawa 2021). For instance, during the mid-growing season, when temperature and precipitation are at their highest, plants

often reach their peak standing leaf area, enabling them to generate large amounts of photosynthates that support root production (Quan et al. 2010). Existing knowledge on the intra-annual patterns of NPP allocation can thus be enhanced by quantifying the seasonal highs and lows of various fine root demographic processes and analyzing the timing of FRP and FRM fluctuations in relation to changes in belowground conditions and nutrient levels.

Aside from the insufficient exploration of intra-annual patterns of FRP and FRM, some likely sources of uncertainty inherent in allometry-based NPP estimation and ingrowth coring are acknowledged. The accuracy of species-specific ΔWB and ΔCRB estimates relies on the applicability of the nationally developed allometric equations to Mt. Gariwang, a landscape with its own distinct set of environmental conditions. Further, ingrowth core installation introduces an unavoidable degree of disturbance to soil bulk density and other physical properties that are crucial for fine root recolonization. Nonetheless, the combined magnitude of these uncertainties, along with natural spatial heterogeneity and measurement-related variability, accounts for at most 9% of our estimated NPP (i.e., 5% for LK, 8% for PD and PK, and 9% for QM), indicating that the observed patterns of NPP distribution across stands are relatively robust. Future studies would benefit from extrapolating woody and coarse root NPP, as well as fine root demographic rates, using integrated sampling approaches to (1) better capture the complexity of these compartments and (2) deepen the mechanistic understanding of the factors governing NPP, its partitioning, and associated carbon fluxes in cool temperate environments.

Conclusions

This study comprehensively characterized ecosystem-level NPP and its allocation patterns in four cool temperate forests existing within a shared geographical and climatic region. Variation in total NPP between deciduous and evergreen stands likely reflects differences in light interception capacity, efficiency in converting solar radiation to dry matter, and distributional constraints on roots and belowground symbionts. Despite these inter-stand differences, all stands consistently allocated a smaller proportion of NPP to belowground growth, demonstrating a common strategy of prioritizing aboveground investment when soil resources are not limiting. Litterfall dynamics, while variable in annual rate across stands, followed a common seasonal pattern peaking in autumn, which closely aligned with the natural foliar phenology of many temperate species. FRP also exhibited considerable stand- and depth-dependent variability that indicates (1) species-specific differences in carbohydrate allocation and supply for root growth, as well as (2) vertical heterogeneity in resource availability and mechanical impedance within the soil profile. These findings collectively contribute to a deeper understanding of forest carbon partitioning, providing insights for refining regional carbon budgets in cool temperate environments.

Supplementary Information

The online version contains supplementary material available at https://doi.org/10.1186/s13717-026-00670-z.

Supplementary material 1.

Acknowledgements
The authors express their appreciation to the members of the Silviculture Laboratory at the Department of Forest Resources, College of Agriculture and Life Sciences, Chungnam National University, for their generous assistance with field and laboratory work.

Author contributions
Min Seon Jo: Data curation, Formal analysis, Methodology, Investigation, Visualization, Writing—original draft. Si Ho Han: Data curation, Formal analysis, Methodology, Investigation, Visualization, Writing—original draft. Mark Bryan Carayugan: Data curation, Formal analysis, Methodology, Investigation, Visualization, Writing—original draft. Julia Inacio Carvalho: Investigation, Validation, Writing—review and editing. Ye Jin Kong: Investigation, Validation, Writing—review and editing. Jong Chan Yeo: Investigation, Writing—review and editing. Lan Thi Ngoc Tran: Investigation, Writing—review and editing. Wencelito Palis Hintural: Validation, Writing—review and editing. S.K. Abidur Rahman: Investigation, Writing—review and editing. Hyun Ju Lee: Validation, Writing—review and editing. Sang Hyun Park: Investigation, Writing—review and editing. Hyung Won Kim: Validation, Writing—review and editing. Yu Seon Lee: Validation, Writing—review and editing. Woo Bin Youn: Validation, Writing—review and editing. Ji Young An: Conceptualization, Methodology, Project administration, Supervision, Writing—review and editing. Byung Bae Park: Conceptualization, Methodology, Project administration, Supervision, Writing—review and editing.

Funding
This study was conducted with the support of the R&D program for Forest Science Technology (Project No. RS-2025-02219895) provided by the Korea Forest Service (Korea Forestry Promotion Institute). This work was also supported by the National Research Foundation of Korea (NRF) grant funded by the Korean government (MSIT) (No.2021R1A2C201017812).

Data availability
The data will be made available upon reasonable request.

Declarations

Ethics approval and consent to participate
Not applicable.

Consent for publication
Not applicable.

Competing interests
The authors declare that they have no competing interests.

Author details
[1]Department of Environment and Forest Resources, College of Agriculture and Life Sciences, Chungnam National University, 99 Daehak-ro, Yuseong-gu, Daejeon 34134, Republic of Korea. [2]Gyeryongsan National Park Office, Korea National Park Service, Gongju 32626, Republic of Korea. [3]Kasuya Research Forest, Kyushu University, Sasaguri, Fukuoka 811-2415, Japan. [4]Forest Ecology Division, National Institute of Forest Science, Seoul 02455, Republic of Korea.

[5]Urban Ecosystem Research Division, Ecosystems Research and Development Bureau, Department of Environment and Natural Resources, 4031 Los Baños, Laguna, Philippines. [6]Forest Environment and Geospatial Technology Research Institute, Sejong 30084, Republic of Korea. [7]Korea Association of Forest Enviro-conservation Technology, Cheongju 28165, Republic of Korea. [8]International Biological Material Research Center, Korea Research Institute of Bioscience and Biotechnology, Daejeon 34141, Republic of Korea. [9]Division of Environmental and Forest Science, College of Agriculture and Life Sciences, Gyeongsang National University, Jinju 52725, Republic of Korea.

Received: 24 July 2025 Accepted: 6 January 2026
Published online: 23 January 2026

References

Addo-Danso SD, Prescott CE, Smith AR (2016) Methods for estimating root biomass and production in forest and woodland ecosystem carbon studies: a review. For Ecol Manage 359:332–351. https://doi.org/10.1016/j.foreco.2015.08.015

Agrawal A, Gopal K (2013) Measurement of primary productivity in relation to food chain. In: Agrawal A, Gopal K (eds) Biomonitoring of Water and Waste Water. Springer India, India, pp 1–13

An JY, Osawa A (2021) Seasonal patterns of fine root dynamics and their contribution to net primary production in hinoki cypress (*Chamaecyparis obtusa*) and konara oak (*Quercus serrata*) forests. Trees 35:255–271. https://doi.org/10.1007/s00468-020-02030-6

An JY, Park BB, Chun JH, Osawa A (2017) Litterfall production and fine root dynamics in cool-temperate forests. PLoS ONE 12:e0180126. https://doi.org/10.1371/journal.pone.0180126

Anees SA, Mehmood K, Rehman A et al (2024) Unveiling fractional vegetation cover dynamics: a spatiotemporal analysis using MODIS NDVI and machine learning. Environ Sustain Indic 24:100485. https://doi.org/10.1016/j.indic.2024.100485

Anees SA, Mehmood K, Luo M et al (2025a) Advancing forest fire burn severity and vegetation recovery assessments using remote sensing and machine learning approaches. Ecol Inform 92:103446. https://doi.org/10.1016/j.ecoinf.2025.103446

Anees SA, Mehmood K, Muhammad S et al (2025b) Spatiotemporal dynamics and environmental drivers of fractional vegetation cover in a semi-arid region using machine learning. Theor Appl Climatol 156:475. https://doi.org/10.1007/s00704-025-05696-5

Aragão LEOC, Malhi Y, Metcalfe DB et al (2009) Above- and below-ground net primary productivity across ten Amazonian forests on contrasting soils. Biogeosciences 6:2759–2778. https://doi.org/10.5194/bg-6-2759-2009

Baldocchi DD, Ma S, Rambal S et al (2010) On the differential advantages of evergreenness and deciduousness in mediterranean oak woodlands: a flux perspective. Ecol Appl 20:1583–1597. https://doi.org/10.1890/08-2047.1

Baul TK, Chowdhury AI, Uddin MJ et al (2021) Forest carbon stocks under three canopy densities in Sitapahar natural forest reserve in Chittagong Hill Tracts of Bangladesh. For Ecol Manage 492:119217. https://doi.org/10.1016/j.foreco.2021.119217

Behera SK, Behera MD, Tuli R (2015) An indirect method of estimating leaf area index in a tropical deciduous forest of India. Ecol Indic 58:356–364. https://doi.org/10.1016/j.ecolind.2015.05.038

Carayugan MB, An JY, Han SH, Park BB (2023) Litterfall and element fluxes in secondary successional forests of South Korea. Ecol Indic 156:111096. https://doi.org/10.1016/j.ecolind.2023.111096

Carayugan MB, An JY, Park BB (2025) Characterizing fine-scale spatiotemporal variations in canopy litterfall and fine root dynamics in cool temperate forest ecosystems. Glob Ecol Conserv 59:e03519. https://doi.org/10.1016/j.gecco.2025.e03519

Carvalho JI, An JY, Tran LTN et al (2025) Root decomposition of four temperate species in the Republic of Korea: associations of root traits and microbial community with root decay. Plant Soil 513:1609–1630. https://doi.org/10.1007/s11104-025-07276-y

Carvalho P, Foulkes MJ (2019) Roots and uptake of water and nutrients. In: Savin R, Slafer GA (eds) Crop Science. Springer, New York, NY, pp 107–130

Clark DA, Brown S, Kicklighter DW et al (2001) Measuring net primary production in forests: concepts and field methods. Ecol Appl 11:356–370. https://doi.org/10.1890/1051-0761(2001)011[0356:MNPPIF]2.0.CO;2

Cordeiro AL, Norby RJ, Andersen KM et al (2020) Fine-root dynamics vary with soil depth and precipitation in a low-nutrient tropical forest in the Central Amazonia. Plant-Environ Interact 1:3–16. https://doi.org/10.1002/pei3.10010

Curiel Yuste J, Konôpka B, Janssens IA et al (2005) Contrasting net primary productivity and carbon distribution between neighboring stands of *Quercus robur* and *Pinus sylvestris*. Tree Physiol 25:701–712. https://doi.org/10.1093/treephys/25.6.701

Doughty CE, Goldsmith GR, Raab N et al (2018) What controls variation in carbon use efficiency among Amazonian tropical forests? Biotropica 50:16–25. https://doi.org/10.1111/btp.12504

Eissenstat DM, Yanai RD (1997) The ecology of root lifespan. Adv Ecol Res 27:1–60

Epron D, Ngao J, Dannoura M et al (2011) Seasonal variations of belowground carbon transfer assessed by in situ $^{13}CO_2$ pulse labelling of trees. Biogeosciences 8:1153–1168. https://doi.org/10.5194/bg-8-1153-2011

Fairley RI, Alexander IJ (1985) Methods of calculating fine root production in forests. In: Ecological interactions in soil: plants, microbes and animals. Blackwell Scientific, Oxford, pp 37–42

Finér L, Helmisaari H-S, Lõhmus K et al (2007) Variation in fine root biomass of three European tree species: beech (*Fagus sylvatica* L.), Norway spruce (*Picea abies* L. Karst.), and Scots pine (*Pinus sylvestris* L.). Plant Biosyst 141:394–405. https://doi.org/10.1080/11263500701625897

Freschet GT, Violle C, Bourget MY et al (2018) Allocation, morphology, physiology, architecture: the multiple facets of plant above- and below-ground responses to resource stress. New Phytol 219:1338–1352. https://doi.org/10.1111/nph.15225

Fukuzawa K, Shibata H, Takagi K et al (2013) Temporal variation in fine-root biomass, production and mortality in a cool temperate forest covered with dense understory vegetation in northern Japan. For Ecol Manage 310:700–710. https://doi.org/10.1016/j.foreco.2013.09.015

Giweta M (2020) Role of litter production and its decomposition, and factors affecting the processes in a tropical forest ecosystem: a review. J Ecol Environ 44:81–89. https://doi.org/10.1186/s41610-020-0151-2

Gower ST, Vogel JG, Norman JM et al (1997) Carbon distribution and aboveground net primary production in aspen, jack pine, and black spruce stands in Saskatchewan and Manitoba, Canada. J Geophys Res Atmos 102:29029–29041. https://doi.org/10.1029/97JD02317

Helmisaari H-S (1992) Nutrient retranslocation in three *Pinus sylvestris* stands. For Ecol Manage 51:347–367. https://doi.org/10.1016/0378-1127(92)90334-6

Jasińska J, Sewerniak P, Puchałka R (2020) Litterfall in a Scots pine forest on inland dunes in Central Europe: mass, seasonal dynamics and chemistry. Forests 11:678. https://doi.org/10.3390/f11060678

Jeong J-Y, Kim C, An H-C et al (2009) A comparison of litterfall dynamics in three coniferous plantations of identical age under similar site conditions. J Ecol Environ 32:97–102. https://doi.org/10.5141/JEFB.2009.32.2.097

Joshi RK, Gupta R, Mishra A, Garkoti SC (2024) Seasonal variations of leaf ecophysiological traits and strategies of co-occurring evergreen and deciduous trees in white oak forest in the central Himalayas. Environ Monit Assess 196:634. https://doi.org/10.1007/s10661-024-12771-3

Jung S-J, Lee CM, Kwon T-S (2013) Effects of forest roads on emipteran diversity in Mt. Gariwang, Korea: test of intermediate disturbance hypothesis. J Asia-Pac Biodivers 6:239–248. https://doi.org/10.7229/jkn.2013.6.2.239

Kang H (1999) Variations in the seed production of *Pinus densiflora* trees. Korean J Biol Sci 3:29–39. https://doi.org/10.1080/12265071.1999.9647462

Kang H (2005) A five-year study of mast seeding in *Pinus densiflora*. J Plant Biol 48:159–169. https://doi.org/10.1007/BF03030404

Keyes MR, Grier CC (1981) Above- and below-ground net production in 40-year-old Douglas-fir stands on low and high productivity sites. Can J For Res 11:599–605. https://doi.org/10.1139/x81-082

Kim M, Koo N, Kim AR et al (2025) Reference ecosystem condition-based syntaxonomic study for ecological restoration and protection of temperate forests in South Korea. Diversity 17:40. https://doi.org/10.3390/d17010040

Lee CM, Kwon T-S, Park YK et al (2014) Diversity of beetles in Gariwangsan Mountain, South Korea: influence of forest management and sampling efficiency

of collecting method. J Asia-Pac Biodivers 7:319–346. https://doi.org/10.1016/j.japb.2014.06.005
Lee CM, Kim S-S, Kwon T-S (2016) Butterfly fauna in Mount Gariwang-san, Korea. J Asia-Pac Biodivers 9:198–204. https://doi.org/10.1016/j.japb.2016.02.005
Li FL, McCormack ML, Liu X et al (2020) Vertical fine-root distributions in five subalpine forest types shifts with soil properties across environmental gradients. Plant Soil 456:129–143. https://doi.org/10.1007/s11104-020-04706-x
Lili Z, Vivek Y, Hengchen Z et al (2024) Climate drivers of litterfall biomass dynamics in three types of forest stands on the Loess Plateau. Ecol Indic 163:112088. https://doi.org/10.1016/j.ecolind.2024.112088
Liu Y, Wang G, Yu K et al (2018) A new method to optimize root order classification based on the diameter interval of fine root. Sci Rep 8:2960. https://doi.org/10.1038/s41598-018-21248-6
Malhi Y, Doughty C, Galbraith D (2011) The allocation of ecosystem net primary productivity in tropical forests. Philos Trans R Soc B Biol Sci 366:3225–3245. https://doi.org/10.1098/rstb.2011.0062
Mehmood K, Anees SA, Muhammad S et al (2025a) Machine learning and spatio temporal analysis for assessing ecological impacts of the Billion Tree Afforestation Project. Ecol Evol 15:e70736. https://doi.org/10.1002/ece3.70736
Mehmood K, Anees SA, Shahzad F et al (2025b) Exploring vegetation health in Southern Thailand under climate stress from temperature and water impacts between 2000 and 2023. Sci Rep 15:30491. https://doi.org/10.1038/s41598-025-16293-x
Mngadi M, Odindi J, Mutanga O, Sibanda M (2022) Estimating aboveground net primary productivity of reforested trees in an urban landscape using biophysical variables and remotely sensed data. Sci Total Environ 802:149958. https://doi.org/10.1016/j.scitotenv.2021.149958
Nakagawa M, Ushio M, Kume T, Nakashizuka T (2019) Seasonal and long-term patterns in litterfall in a Bornean tropical rainforest. Ecol Res 34:31–39. https://doi.org/10.1111/1440-1703.1003
National Institute of Agricultural Sciences. Soil Environment Map. https://soil.rda.go.kr/. Accessed 3 Jul 2025
Ochoa-Hueso R, Piñeiro J, Power SA (2020) Spatial distribution of fine root biomass in a remnant *Eucalyptus tereticornis* woodland in Eastern Australia. Plant Ecol 221:55–62. https://doi.org/10.1007/s11258-019-00990-5
Ostonen I, Lõhmus K, Pajuste K (2005) Fine root biomass, production and its proportion of NPP in a fertile middle-aged Norway spruce forest: comparison of soil core and ingrowth core methods. For Ecol Manage 212:264–277. https://doi.org/10.1016/j.foreco.2005.03.064
Quan X, Wang C, Zhang Q et al (2010) Dynamics of fine roots in five Chinese temperate forests. J Plant Res 123:497–507. https://doi.org/10.1007/s10265-010-0322-9
Singh N, Parida BR, Charakborty JS, Patel NR (2019) Net ecosystem exchange of CO_2 in deciduous pine forest of lower western Himalaya, India. Resources 8:98. https://doi.org/10.3390/resources8020098
Smithwick EAH, Lucash MS, McCormack ML, Sivandran G (2014) Improving the representation of roots in terrestrial models. Ecol Model 291:193–204. https://doi.org/10.1016/j.ecolmodel.2014.07.023
Son YM, Kim RH, Lee KH et al (2014) Carbon emission factors and biomass allometric equations by species in Korea. National Institute of Forest Science, Seoul, Republic of Korea
Song Y, Zhang M, Guo Y, Gao X (2023) Change in seed dormancy status controls seasonal timing of seed germination in Korean pine (*Pinus koraiensis*). J Plant Ecol 16:rtac067. https://doi.org/10.1093/jpe/rtac067
Streiff L (2021) NASA satellites help quantify forests' impacts on global carbon budget. National aeronautics and space administration
Sun X, Liu F, Zhang Q et al (2021) Biotic and climatic controls on the interannual variation in canopy litterfall of a deciduous broad-leaved forest. Agric For Meteorol 307:108483. https://doi.org/10.1016/j.agrformet.2021.108483
Tang G, Beckage B, Smith B, Miller PA (2010) Estimating potential forest npp, biomass and their climatic sensitivity in New England using a dynamic ecosystem model. Ecosphere 1:art18. https://doi.org/10.1890/ES10-00087.1
Tateno R, Hishi T, Takeda H (2004) Above- and belowground biomass and net primary production in a cool-temperate deciduous forest in relation to topographical changes in soil nitrogen. For Ecol Manage 193:297–306. https://doi.org/10.1016/j.foreco.2003.11.011
Tomlinson KW, van Langevelde F, Ward D et al (2013) Deciduous and evergreen trees differ in juvenile biomass allometries because of differences in allocation to root storage. Ann Bot 112:575–587. https://doi.org/10.1093/aob/mct132
Tran LT, An JY, Carayugan MB et al (2024) Fine-root distribution and soil physico-chemical property variations in four contrasting urban land-use types in South Korea. Plants 13:164. https://doi.org/10.3390/plants13020164
Van Do T, Sato T, Saito S, Kozan O (2015) Fine-root production and litterfall: main contributions to net primary production in an old-growth evergreen broad-leaved forest in southwestern Japan. Ecol Res 30:921–930. https://doi.org/10.1007/s11284-015-1295-x
Vogt KA, Vogt DJ, Palmiotto PA et al (1995) Review of root dynamics in forest ecosystems grouped by climate, climatic forest type and species. Plant Soil 187:159–219. https://doi.org/10.1007/BF00017088
Wang CG, Zheng XB, Wang AZ et al (2021) Temperature and precipitation diversely control seasonal and annual dynamics of litterfall in a temperate mixed mature forest, revealed by long-term data analysis. J Geophys Res Biogeosci 126:e2020JG006204. https://doi.org/10.1029/2020JG006204
Wright SJ, Yavitt JB, Wurzburger N et al (2011) Potassium, phosphorus, or nitrogen limit root allocation, tree growth, or litter production in a lowland tropical forest. Ecology 92:1616–1625. https://doi.org/10.1890/10-1558.1
Wurzburger N, Wright SJ (2015) Fine-root responses to fertilization reveal multiple nutrient limitation in a lowland tropical forest. Ecology 96:2137–2146. https://doi.org/10.1890/14-1362.1
Xiao C-W, Yuste JC, Janssens IA et al (2003) Above- and belowground biomass and net primary production in a 73-year-old Scots pine forest. Tree Physiol 23:505–516. https://doi.org/10.1093/treephys/23.8.505
Xie L, Lin G, Wang Q-W, Yin C (2024) Tree species-specific differences in carbon allocation to ectomycorrhizal symbionts tightly relate to ectomycorrhizal fungal community composition. For Ecol Manage 562:121935. https://doi.org/10.1016/j.foreco.2024.121935
Yuan ZY, Chen HYH (2013) Simplifying the decision matrix for estimating fine root production by the sequential soil coring approach. Acta Oecol 48:54–61. https://doi.org/10.1016/j.actao.2013.01.009
Zhang H, Yuan W, Dong W, Liu S (2014) Seasonal patterns of litterfall in forest ecosystem worldwide. Ecol Complex 20:240–247. https://doi.org/10.1016/j.ecocom.2014.01.003
Zhang M, Chen S, Jiang H et al (2020) The impact of intensive management on net ecosystem productivity and net primary productivity of a Lei bamboo forest. Ecol Model 435:109248. https://doi.org/10.1016/j.ecolmodel.2020.109248
Zhao M, Zhang Q, Li Y et al (2025) Unraveling biological characteristics of flower bud differentiation and reproductive organ development, advancing genetic improvement and ameliorating cone yield in *Pinus koraiensis*. Ind Crops Prod 227:120815. https://doi.org/10.1016/j.indcrop.2025.120815
Zheng G, Su X, Chen X et al (2024) Variations in fine root biomass, morphology, and vertical distribution in both trees and understory vegetation among Chinese fir plantations. For Ecol Manage 557:121748. https://doi.org/10.1016/j.foreco.2024.121748
Zhou Y, Su J, Janssens IA et al (2014) Fine root and litterfall dynamics of three Korean pine (*Pinus koraiensis*) forests along an altitudinal gradient. Plant Soil 374:19–32. https://doi.org/10.1007/s11104-013-1816-8
Zhou L, Li S, Liu B et al (2019) Tissue-specific carbon concentration, carbon stock, and distribution in *Cunninghamia lanceolata* (Lamb.) Hook plantations at various developmental stages in subtropical China. Ann For Sci 76:70. https://doi.org/10.1007/s13595-019-0851-x
Zhu X, Zou X, Lu E et al (2021) Litterfall biomass and nutrient cycling in karst and nearby non-karst forests in tropical China: a 10-year comparison. Sci Total Environ 758:143619. https://doi.org/10.1016/j.scitotenv.2020.143619
Zhuang L, Yang W, Wu F et al (2018) Diameter-related variations in root decomposition of three common subalpine tree species in southwestern China. Geoderma 311:1–8. https://doi.org/10.1016/j.geoderma.2017.09.041

Publisher's Note

Springer Nature remains neutral with regard to jurisdictional claims in published maps and institutional affiliations.